EFFECT OF TEMPERATURE DIFFERENCE ACROSS ORC BOILER ON THE THERMAL STORAGE MEDIUM COST IN A SOLAR ORC

Abhishek N. Kshirsagar[1], Pardeep Garg[2†], Pramod Kumar[2#], Matthew S. Orosz[3]

[1]Pune Vidyarthi Griha's College of Engineering and Technology
Vidyanagari, Pune, Maharashtra, India
E-mail: kshirsagar_abhishek@yahoo.com

[2]Indian Institute of Science Bangalore
C V Raman Ave, Bengaluru, Karnataka, India
[†]E-mail: pardeep_1127@yahoo.com
[#]E-mail: pramod_k24@yahoo.com

[3]Massachusetts Institute of Technology
Cambridge, MA, USA
E-mail: mso@mit.edu

ABSTRACT

This paper identifies the key parameters to be optimized on a thermo-economic basis in a solar-ORC to minimize the storage cost associated with it. These parameters are ORC working fluid, its operating conditions and the heat transfer fluid used. A case study of a pebble bed thermal energy storage system is carried out using two working fluids in a 100 kWe ORC namely, R-245fa and R-134a for a wide range of expander inlet temperatures. Heat transfer fluids considered are ethylene glycol (for temperatures < 180 °C), Therminol VP-1 and Glycerol (for temperatures > 180 °C). Effect of these parameters is evaluated for the case scenario of suppressing the fluctuations in the ORC side arising due to solar insolation calculated using ASHRAE clear sky model. For a given energy storage, HTF temperature difference across the boiler and HTF mass required for storage and hence cost of PB-TES system are reported to be inversely co-related. Higher expander inlet temperatures in case of R134a ORC with Glycerol as an HTF are found to yield the lowest storage cost.

1. INTRODUCTION

Organic Rankine cycle (ORC) technology can be integrated with geothermal (Astolfi et al., 2014) or process heat available from industry (Wei et al. 2007) or renewable energy source such as a concentrated solar thermal system using parabolic trough collectors (Quoilin et al., 2011). In case when ORCs are directly coupled with solar, issues arising due to fluctuating nature of solar insolation are reported to adversely affect the ORC performance (Twomey et al., 2013). Thermal storage in this regard can help in suppressing the fluctuations and also provide an option for power generation during non-solar hours (Taljan et al. 2012). There exist a number of storage technologies which need to be optimized for the minimum cost depending on the application. In such a study, Herrmann and Kearney (2002) came up with a techno-economic analysis for the various existing storage technologies and emphasized on the need of reducing the cost of storage media. One possible way to reduce the cost of storage medium is to store partial amount of heat in the inexpensive rocks or pebbles as suggested by Meier et al., 1991. The technology is analyzed in a great detail by a number of researchers (Hasnain et al. 1998; Mawire et al., 2009; Singh et al, 2010 and Zanganeh et al., 2012) and simple modeling techniques are proposed. However, literature lacks the work on optimizing the cost of storage in conjunction with the ORC.

This paper analyzes the effect of ORC working fluid and its operating conditions on the cost associated with the pebble bed based thermal energy storage (PB-TES) tank designed to die out the fluctuations arising due to varying solar insolation. In this regard, a procedure is developed to calculate the mass of HTF required in a PB-TES tank. HTF temperature difference across the boiler and the mass of HTF stored in a PB-TES tank (hence the cost of the storage system) are observed to be inversely co-related. This temperature difference in turn is found to be dependent on ORC working fluid and its operating conditions. The same is illustrated in a great detail for the two different working fluids in ORC namely, R245fa and R134a for different operating conditions in the power block.

2. SOLAR-ORC DETAILS

Physical layout of the solar-ORC considered in this paper consists of two closed loops, a) heat transfer fluid (HTF) and b) working fluid loop as shown in Fig. 1. In the HTF loop, cold HTF from a PB-TES is pumped to a parabolic trough collector where it gets heated up and is then sent for the storage in a PB-TES tank. Working fluid loop is a regenerative ORC where the expander exhaust heat is recovered to heat up the pump outlet fluid. The two loops interact via a heat exchanger termed as an HEX (boiler for the working fluid) in this paper where the HTF coming from a PB-TES tank is cooled and working fluid in turn is heated up to the expander inlet temperature.

2.1 ORC details

Low pressure and low temperature liquid at state 1_{wf} is pumped to higher pressures (state 2_{wf}). High pressure fluid at this state is preheated in a regenerator from state 2_{wf} to 5_{wf} by recovering heat from expander exhaust wherein the low pressure gas is cooled from state 4_{wf} to 6_{wf}. Remaining heat addition from state 5_{wf} to 3_{wf} occurs in a heater via a heat transfer fluid (HTF). Working fluid is then further expanded in a scroll device till state 4_{wf}. Regenerator outlet on low pressure side (state 6_{wf}) is then cooled in an air cooled condenser till state 1_{wf} to complete the cycle. Ideally, the pumping and expansion processes should be isentropic and heat transfer processes isobaric which in reality tend to deviate. Modeling details for such an ORC could be found in (Garg et al., 2013) and for the sake of completeness are repeated here.

i. Power generation is 100 kWe.

ii. Minimum cycle temperature (T_1) is 45 °C.

iii. Pump efficiency is 90 %.

iv. Expander efficiency is 65 %.

v. Pinch temperature in the regenerator and the HEX is set at 10 °C and the flow arrangement is counter flow type.

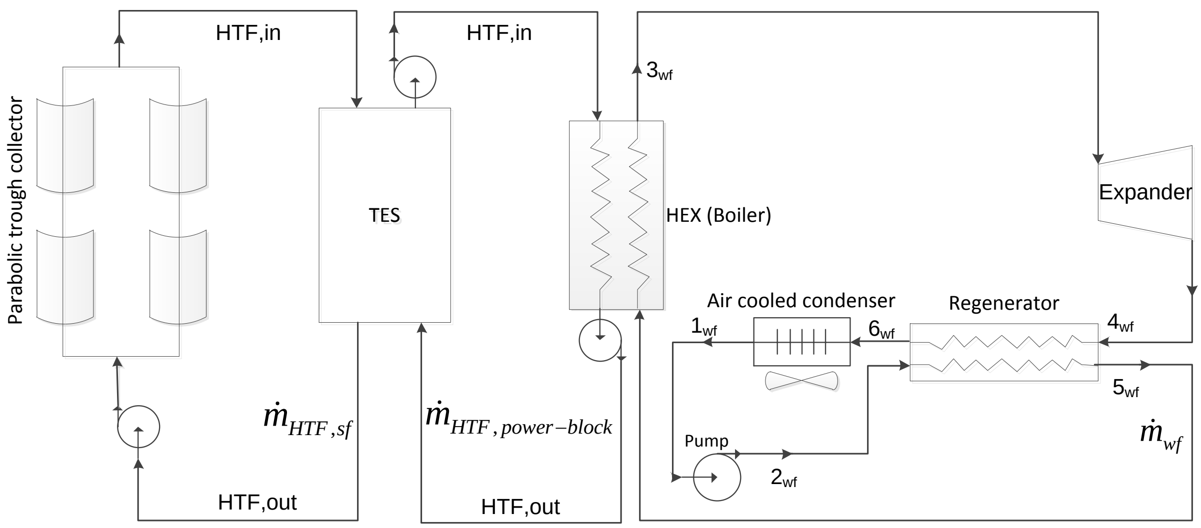

Figure 1: Schematic of an ORC

2.2 TES details

Heated HTF from solar field enters the PB-TES tank from the top where it loses heat to the pebbles and the cold HTF around. The same amount of cold HTF leaves the tank from the bottom side and is passed to the solar collectors to heat it up again. Control strategy followed in this loop is to regulate HTF mass flow rate to achieve steady HTF temperatures (also equal to HTF maximum temperature). In another loop, hot HTF from the PB-TES is passed on to the HEX (boiler for the working fluid) where it supplies the heat to the working fluid in the power block. Storage sizing is done in such a way that the fluctuations arising due to solar insolation are damped out, thus, ensuring the steady HTF operating conditions and ORC operation at its designed conditions throughout the day.

3. METHODOLOGY

To calculate the solar PB-TES costs associated with the ORC algorithm given in Fig. 2 is considered. Firstly, the ORC for the given operating expander inlet temperature is designed for the best efficiency. Solar insolation or DNI calculations are performed using ASHRAE clear sky model for which the details can be found in Appendix A. TES is modeled in such a way that temperature drop across the HTF in HEX and PB-TES are identical. In turn, these inlet and outlet temperatures of the PB-TES are governed by the operating conditions on working fluid side in power block discussed in detail in ahead.

3.1. Mass of storage media required

A bottom-up approach is followed to calculate the storage needs of a solar-ORC to damp the fluctuations in the operating conditions in the power block. Firstly, HTF operating conditions across the HEX i.e. HTF inlet and outlet temperature are calculated.

Calculation of HTF operating conditions in HEX

The procedure to calculate HTF operating conditions is based on pinch point analysis in the HEX. It is observed that pinch point in the HEX occurs at the liquid saturation line of the working fluid as shown in Fig. 4.

$$T_{HTF,pinch} = T_{2f,wf} + \Delta T_{pinch} \tag{1}$$

Further, to minimize the HEX irreversibility (Garg et al., 2013),

$$T_{HTF,in} = T_{3,wf} + \Delta T_{pinch} \tag{2}$$

Applying 1st law of thermodynamics to control volume across state 2_{wf} and 3_{wf}

$$\dot{m}_{HTF} c_{p,HTF} (T_{HTF,in} - T_{HTF,pinch}) = \dot{m}_{wf} (h_{3_{wf}} - h_{2f_{wf}}) \tag{3}$$

Having defined the thermodynamic properties on working fluid as well as HTF side, one can calculate the product of mass flow rate and specific heat of HTF

$$\dot{m}_{HTF} c_{p,HTF} = \frac{\dot{m}_{wf} (h_{3_{wf}} - h_{2f_{wf}})}{(T_{HTF,in} - T_{HTF,pinch})} \tag{4}$$

Once the above product is known , application of 1st law to the HEX can be applied to calculate the $T_{HTF,in}$

$$\dot{m}_{HTF} c_{p,HTF} (T_{HTF,in} - T_{HTF,out}) = \dot{Q}_{power-block} \tag{5}$$

Simplifying the above equation for $T_{HTF,out}$

$$T_{HTF,out} = T_{HTF,in} - \frac{\dot{Q}_{power-block}}{\dot{m}_{HTF} c_{p,HTF}} \tag{6}$$

where, heat required in the power block is

$$\dot{Q}_{power-block} = \frac{\dot{P}}{\eta_{ORC}} \tag{7}$$

For the transcritical cycle above mention procedure is modified to calculate $T_{HTF,out}$.

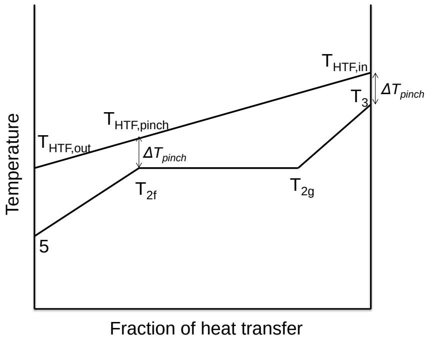

Figure 2. Temperature profiles of HTF and working fluid in a typical HEX.

PB-TES design

Let A_{solar} be the area of solar field required to generate power output ($\dot{P}$) for the full solar-day duration. Then, heat available from the collector whose efficiency is $\eta_{collector}$ is

$$\dot{Q}_{collector} = \eta_{collector} DNI_N A_{solar} \tag{8}$$

On a given day variation of $\dot{Q}_{collector}$ (derived using ASHRAE clear sky model with a cloud factor) with time is presented in Figure 3 along with $\dot{Q}_{power-block}$ which is steady in nature. Solar field area is designed in such a way that area under both the curves is identical. Mathematically,

$$\text{area(ABCD)} = \text{area(AGHD)} \tag{9}$$

or

$$\dot{Q}_{power-block} \Delta t_h = \int_{t_{1h}}^{t_{4h}} \dot{Q}_{collector} \, dt_h \tag{10}$$

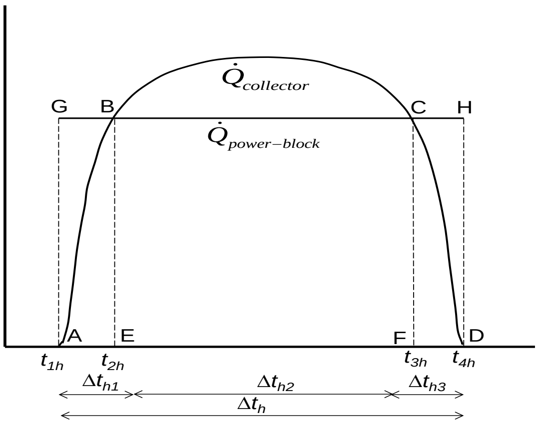

Figure 2: A standard DNI curve taken with constant output power

It can be noted that heat available from the collector exceeds that of required in the power block in the hours between t_{2h} to t_{3h} and can be stored in the PB-TES. The stored heat can then later be used in the hours between t_{1h} to t_{2h} and t_{3h} to t_{4h} when the heat available from the collector is not enough to run the power block. It can be appreciated that heat stored in the surplus hours should be equal to energy used in the deficit hours for the steady operation of power block. Energy that needs to be stored in the PB-TES is thus given as

$$\Delta E_{PB-TES} = \text{area}(arc(BC)) - \text{area}(BCFE) \tag{11}$$

Or

$$\Delta E_{PB-TES} = \int_{t_{2h}}^{t_{3h}} \dot{Q}_{collector} dt_h - \dot{Q}_{power-block} \Delta t_{3h} \tag{12}$$

Further, this energy is stored in pebbles as well as HTF

$$\Delta E_{PB-TES} = \Delta E_{HTF} + \Delta E_{Pebble} \tag{13}$$

where,

$$\Delta E_{HTF} = M_{HTF} c_{p_{HTF}} \Delta T_{HTF} \tag{14}$$

$$\Delta E_{Pebble} = M_{Pebble} c_{p_{Pebble}} \Delta T_{Pebble} \tag{15}$$

Further, condition of local thermal equilibrium is assumed to be valid in the PB-TES which makes the temperature of HTF and pebble equal. Break up of ΔE_{PB-TES} is given by Eq. 10 in the form of the porosity ($\varphi = V_{HTF}/V_{Total}$) in the tank.

$$\Delta E_{PB-TES} = (\varphi \rho_{HTF} c_{p\ HTF} + (1-\varphi)\rho_{Pebble} c_{p\ Pebble}) V_{Total} \Delta T_{HTF} \tag{16}$$

Knowing the value of ΔT_{HTF} and thermo-physical properties of the storage media, V_{Total} can be calculated. Eqs. (7), (10) and (4) are simplified to obtain M_{HTF}

$$M_{HTF} = \frac{\Delta E_{PB-TES}}{c_{p\ HTF} \Delta T_{HTF}} - M_{Pebble} \frac{c_{p_{Pebble}}}{c_{p\ HTF}} \tag{17}$$

Above equation establishes an inverse relationship between M_{HTF} and ΔT_{HTF} indicating the storage cost to be a strong function of working fluid in ORC and its operating conditions.

3.2. Storage Media properties

Pebble type considered here is fused silica with density of 2200 kg/m^3 and specific heat of 740 J/kgK. Three different HTFs are considered, namely Ethylene Glycol, Therminol VP1 and Glycerol. For HTF operating temperatures lower than 180 °C, Ethylene Glycol is considered otherwise Therminol VP1 and Glycerol. Though, thermo-physical properties of HTFs are assumed to be the function of temperature as given in the Appendix B along with the cost functions, for the given operating conditions of HTF, thermo-physical properties are taken to be the average of those at inlet and outlet temperatures of HTF across HEX.

3.2.1 Assumptions:

i. Pinch temperature in the HEX is 10 °C.

ii. Porosity is taken as 0.45.

iii. While the minimum cycle temperature is fixed at 45 °C, the maximum cycle temperature is considered to be variable.

iv. In case when cycle efficiency becomes asymptote to the pressure ratio at a given expander inlet temperature, to avoid unnecessary high pressure ratio without having a substantial gain in efficiency, the optimum efficiency is chosen corresponding to a pressure ratio where

$$\left.\frac{\partial \eta}{\partial pr}\right|_{T_{3wf}} = 0.005 \tag{18}$$

4. RESULTS AND DISCUSSIONS

The storage model developed above is generic in nature and can be applied to any working fluid. However, the present paper considers R245fa and R134a to perform a detailed comparison in terms of the storage cost. Storage cost for the rest of the working fluids is found to be somewhere between the cost of these two fluids and hence not presented. ORCs are designed in such a way that they operate at maximum efficiencies at the given expander inlet temperature. In this regard, the optimum pressure ratios in the cycle are plotted in Figure 3. It also shows the variation of optimum efficiency corresponding to pressure ratios with the expander inlet temperature for both the working fluids. In case of R245fa, optimum pressure ratio continues to increase with expander inlet temperature whereas in R134a the limit of 60 bar imposed on the high side pressure of the cycle is achieved and hence constant pressure ratios are observed for the temperatures beyond 200°C. Also, the property data available in Refprop (Lemmon et al.) for R134a restricts its use in the ORC to 220 °C in comparison to 260 °C as observed in case of R245fa.

It can also be noticed that beyond ~ 140 °C, ORC efficiency increases almost linearly with expander temperature. Also, cycle efficiency is slightly lower (about 2-3 %) for R134a than R245fa under identical operating conditions which might result in higher storage needs as shown in Figure 4. Further, the storage requirements come down with expander inlet temperature because of higher cycle efficiencies.

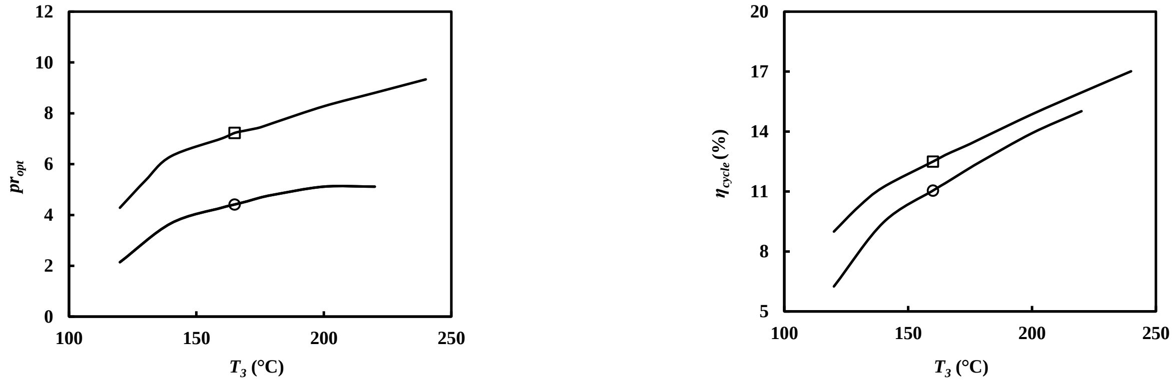

Figure 3: Variation of optimum pressure ratio and optimum efficiency in the ORCs with R245fa and R134a against the expander inlet temperature. Legend: □ R245fa, ○ R134a

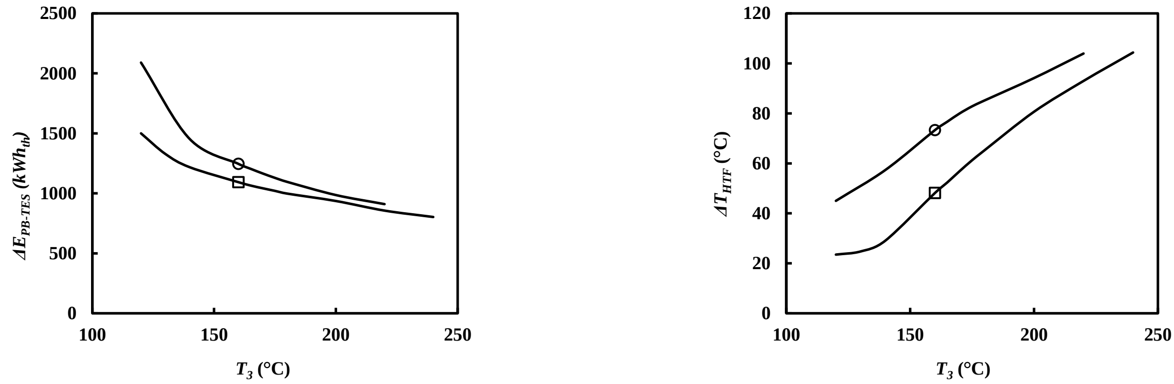

Figure 4: Thermal energy to be stored in PB-TES and HTF temperature difference across the HEX for ORCs with R245fa and R134a against the expander inlet temperature. Legend: □ R245fa, ○ R134a

Another important parameter which has a strong effect on storage namely temperature difference across HTF in the HEX (also across the PB-TES) is also plotted in Figure 4 for the corresponding operating conditions mentioned in the above figures. It is observed that ΔT_{HTF} increases with expander inlet temperature thought the trend is found to be non-linear. The increase in ΔT_{HTF} with temperature can be explained on the basis of the fact that with increase in expander inlet temperature, optimum pressure ratio increases which lowers the amount of latent heat involved in the HEX. In an ideal counter flow HEX, where there is no change in the ratio of specific heats of the two fluids (HTF and working fluid) with respect to the heat transferred in it, the temperature profiles of the both fluids tend to remain parallel and the maximum temperature difference would be observed across HTF. This situation is generally realized in Brayton cycles (Garg et al., 2014) where irreversibility generation is also found to be lower. Further, lower latent heat or no phase change involved in case of R134a in reference to R245fa makes ΔT_{HTF} higher for the former which could potentially reduce the storage cost.

Having known the ΔT_{HTF} and *ΔEPB-TES*, the cost associated with the PB-TES can be calculated which is plotted in Figure 5. Notable observations are as follows:

i. Storage cost as expected is a strong function of HTF type. Glycerol results in the lowest storage costs because of its lower cost per unit mass.

ii. For the given HTF, the storage cost keeps coming down with the expander inlet temperature because of higher cycle efficiency and higher ΔT_{HTF}.

iii. Lowest storage cost is observed for R245fa at the expander inlet temperature 250 °C with Glycerol as an HTF.

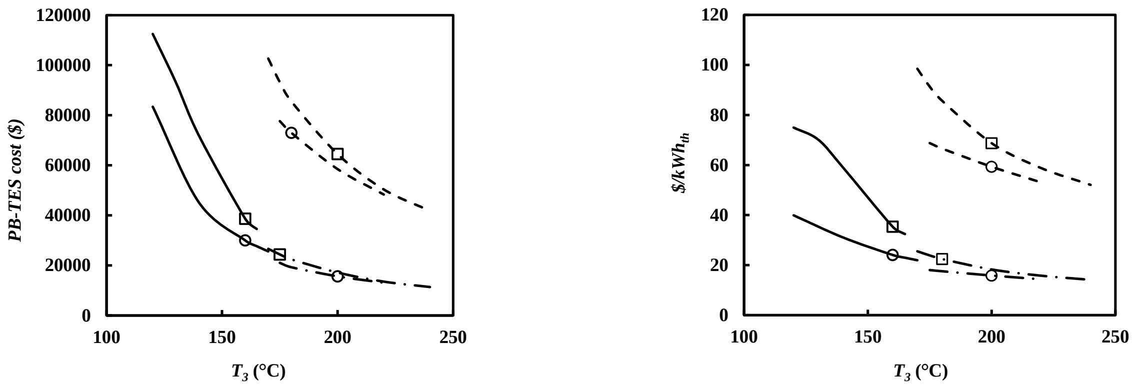

Figure 5: Variation of cost of PB-TES and cost of storage per unit of energy stored in the ORCs with R245fa and R134a against the expander inlet temperature. Legend: □ R245fa, ○ R134a, ——— Ethylene Glycol, —— • —— • —— Glycerol, — — — — Therminol VP1.

Further, the most sought after parameter in storage which is the storage cost per unit of thermal energy stored is also plotted in Figure 5. At any given expander inlet temperature, R134a shows the minimum cost per unit of energy stored in the PB-TES.

5. CONCLUSION

Paper analyzes the cost associated with the pebble bed based thermal energy storage system for the ORCs. A number of parameters are identified which can significantly affect the storage cost for example, HTF type, working fluid type and operating conditions in the ORC. A case study performed on the storage details for R134a and R245fa as working fluids in the ORC predicts the lower cost of storage for the formed in absolute terms as well as on the parameter of cost per unit of energy stored in. The lowest cost per unit of energy is found to be ~14 $/kWh$_{th}$ which includes the cost of the HTF, pebbles and the tank. Further, this study can be extended to a number of working fluids in the ORC and various other HTFs possible with different operating temperature ranges to find the minimum storage cost.

REFERENCES

Garg P., Kumar P., Srinivasan K., Dutta P., 2013, Evaluation of carbon dioxide blends with isopentane and propane as working fluids for organic Rankine cycles, *Applied Thermal Engineering*, Vol. 52, pp 439-448.

Gregor Taljan, Gregor Verbi, Milos Pantos, Manfred Sakulin, Lothar Fickert, 2012, Optimal sizing of biomass-fired Organic Rankine Cycle CHP system with heat storage, *Renewable Energy*, vol. 41 p. 29-38

Ulf Herrmann, David W. Kearney, 2002, Survey of Thermal Energy Storage for Parabolic Trough Power Plants, *Journal of Solar Energy Engineering*, Vol. 124/145-152

G. Zanganeh, A. Pedretti, S. Zavattoni, M. Barbato, A. Steinfeld, 2012, Packed-bed thermal storage for concentrated solar power – Pilot-scale demonstration and industrial-scale design, *Solar Energy*, vol. 86 p. 3084–3098

Mawire, M. McPherson, 2009, Experimental and simulated temperature distribution of an oil-pebble bed thermal energy storage system with a variable heat source, *Applied Thermal Engineering*, vol. 29 p. 1086–1095A.

Hasnain SM. Review on sustainable thermal energy storage technologies. Part1. Heat storage materials and techniques, *Energy Convers Manage*, J1998;39(11):1127–38

Quoilin, S., Orosz, M., Hemond, H., Lemort, V., 2011, Performance and design optimization of a low-cost solar organic Rankine cycle for remote power generation, *Solar Energy*, vol. 85, no. 5: p. 955-966.

Orosz, M. S., 2012, ThermoSolar and photovoltaic hybridization for small scale Distributed Generation: Applications for Powering Rural Health, Doctoral dissertation, Massachusetts Institute of Technology.

Orosz, M. S., Quoilin, S., Hemond, H., Sorce: A Design Tool For Solar Organic Rankine Cycle Systems In Distributed Generation Applications Curran, H. M., 1993, Mechanical systems and components, *In:*Lof, G. O. G., *Active Solar Systems*, MIT Press, Cambridge, MA: p. 693-94

Appendix A

The following model is used to calculate the DNI for a given location and at any time *t*for which a number of concerned terms are defined for the sake of completeness.

i. Hour angle, ω

$$\omega = (t - 12)15° \tag{A.1}$$

ii. Declination angle, δ

$$\delta = 23.45 \sin\left(\frac{360}{365}(284+n)\right) \tag{A.2}$$

iii. Solar altitude angle, β

$$\sin\beta = \cos l . \cos\omega . \cos\delta + \sin l . \sin\delta \tag{A.3}$$

iv. Solar azimuth angle, ϕ

$$\cos\phi = \frac{\sin\delta . \cos l - \cos\delta . \sin l . \cos\omega}{\cos\beta} \tag{A.4}$$

v. Wall solar azimuth, γ

$$\gamma = |\phi| \tag{A.5}$$

vi. Angle of incidence, θ

$$\cos\theta = \cos\beta . \cos\gamma . \sin\alpha + \sin\beta . \cos\alpha \tag{A.6}$$

vii. Normal direct irradiation, G_{ND}

$$G_{ND} = \frac{A}{\exp\left(\frac{B}{\sin\beta}\right)} C_N \tag{A.7}$$

Where C_N clearness number and constants A and B are are referred from the data provided in the ASHRAE clear sky model handbook.

viii. Direct insolation available on the horizontal surface, DNI_H i.e. without axis tracking

$$DNI_H = G_{ND} . \max(\cos\theta, 0) \tag{A.8}$$

ix. Direct insolation available in the direction normal to sun, DNI_N i.e. with single axis tracking

$$DNI_N = \frac{DNI_H}{\cos\omega} \tag{A.9}$$

Above equation is used to calculate the direct insolation available on the parabolic trough for a clearness coefficient of 0.6.

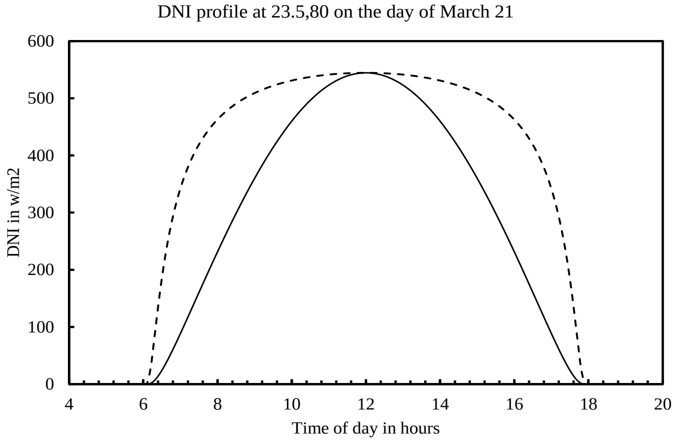

Figure A.1: The above figure shows the DNI profile Sinora, India (23.5, 80), on the day of vernal equinox. ——— Represents DNI without axis tracking and – – – – – represents DNI with single axis tracking.

Appendix B

Therminol VP-1

$$c_{p,HTF} = 1498 + 24.14 \times 10^{-4} T_{HTF,avg} + 59.9 \times 10^{-3} T_{HTF,avg}^2 - 29.879 \times 10^{-5} T_{HTF,avg}^3 + 44.172 \times 10^{-8} T_{HTF,avg}^4$$

$$\rho_{HTF} = 1083.25 - 90.797 \times 10^{-2} T_{HTF,avg} + 7.8116 \times 10^{-4} T_{HTF,avg}^2 - 2.36710^{-6} T_{HTF,avg}^3$$

$$cost_{HTF} = 2 \text{ \$/kg}$$

Ethylene Glycol

$$c_{p,HTF} = 2279.98862 + 4981.34 \times 10^{-3} T_{HTF,avg}$$

$$\rho_{HTF} = 1106.2 + 132.5 \times 10^{-3} T_{HTF,avg} - 8.7 \times 10^{-3} T_{HTF,avg}^2 - 0.02 \times 10^{-3} T_{HTF,avg}^3$$

$$cost_{HTF} = 6 \text{ \$/kg}$$

Glycerol

$$c_{p,HTF} = 2274.87 + 470.71 \times 10^{-3} T_{HTF,avg}$$

$$\rho_{HTF} = 1277 - 65.4 \times 10^{-2} T_{HTF,avg}$$

$$cost_{HTF} = 1.5 \text{ \$/kg}$$

$$cost_{tank} = 130 V_{tank} + 1140$$

NOMENCLATURE

l	Latitude	(º)
ω	Hour angle	(º)
n	Day number	(-)
δ	Declination	(º)
β	Solar altitude angle	(º)
φ	Solar azimuth angle	(º)
γ	Surface solar azimuth angle	(º)
θ	Angle of incidence	(º)

α	Tilt angle	(º)
A	Apparent solar irradiation at air mass equal to zero	(W/m^2)
B	Atmospheric extinction coefficient	(-)
C_N	Clearness number	(-)
T	Temperature	(K)
M	Mass	(kg)
E	Energy	(J)
V	Volume	(m^3)
$A_{collector}$	Area of collector field	(m^2)
$\dot{Q}$	Power	(W)
$\dot{P}$	Output power	(W)
t	Time	(Hours)
c_p	Specific heat	(J/kgK)
η	Efficiency	(-)
ρ	Density	(kg/m^3)
$\dot{m}$	Mass flow rate	(kg/s)
φ	Porosity	(-)

Subscript

h	hour
HTF	heat transfer fluid
Pebbles	pebble
PB-TES	pebble bed thermal energy storage
power-block	power block
collector	collector
Total	total tank
wf	working fluid

Abbreviations

TES	thermal energy storage
HTF	heat transfer fluid
DNI	direct normal insolation
PB-TES	pebble-bed thermal energy storage
ORC	organic Rankine cycle
HEX	heat exchanger

ACKNOWLEDGEMENT

This research is based upon work supported by the Solar Energy Research Institute for India and the U.S. (SERIIUS) funded jointly by the U.S. Department of Energy subcontract DE AC36-08G028308 (Office of Science, Office of Basic Energy Sciences, and Energy Efficiency and Renewable Energy, Solar Energy Technology Program, with support from the Office of International Affairs) and the Government of India subcontract IUSSTF/JCERDC-SERIIUS/2012 dated 22nd Nov. 2012.